—Original—

Protein expression pattern in cerebellum of Cav2.1 mutant, tottering-6j mice

Tae Yeon KIM, Kimie NIIMI, and Eiki TAKAHASHI

Research Resources Center, RIKEN Brain Science Institute 2-1 Hirosawa, Wako, Saitama 351-0198, Japan

Abstract: Neuronal voltage-gated Cav2.1 channel controls a broad array of functions, including neurotransmitter release, neuronal excitability, activity-dependent gene expression, and neuronal survival. The Cav2.1 channel is molecular complexes consisting of several subunits: α1, $α_2/δ$, β, and γ. The pore-forming subunit, α1, is encoded by the *Cacna1a* gene. Tottering-6j mice, generated by the Neuroscience Mutagenesis Facility at The Jackson Laboratory, are a recessive mutant strain in which the mutation has been chemically induced by ethylnitrosourea. In tottering-6j mice, mutation in the *Cacna1a* gene results in a base substitution (C-to-A) in the consensus splice acceptor sequence, which results in deletion of a part of the S4-S5 linker, S5, and a part of S5-S6 linker domain I in the α1 subunit of Cav2.1 channel. The mice display motor dysfunctions and absence-like seizures. However, protein expression in the cerebellum of tottering-6j mice has not been investigated. Real-time quantitative reverse transcription polymerase chain reaction and histological analyses of the cerebellum of tottering-6j mice revealed high expression levels of tyrosine hydroxylase, zebrin II, and ryanodine receptor 3 compared with those of wild-type mice. Conversely, a low level of calretinin expression was found compared with wild-type mice. These results indicate that *Cacna1a* mutation plays a significant role in protein expression patterns and that the tottering-6j mouse is a useful model for understanding protein expression mechanisms.

Key words: *Cacna1a*, Cav2.1α1 subunit, cerebellum, expression, tottering-6j mice

Introduction

Neuronal voltage-gated Ca^{2+} channels (VGCCs) control a broad array of functions, including neurotransmitter release, neurite outgrowth, synaptogenesis, neuronal excitability, and activity-dependent gene expression, in addition to neuronal survival, differentiation, and plasticity [22]. VGCCs are a molecular complex consisting of several subunits, including α1, $α_2/δ$, β, and γ [1]. VGCCs are classified into five groups: Cav1 (L-type), Cav2.2 (N-type), Cav2.1 (P/Q-type), Cav2.3 (R-type), and Cav3 (T-type). The pore-forming α1 subunit has four homologous transmembrane domains (I-IV) with six transmembrane α-helices (S1–S6) and a pore-forming P-loop between S5 and S6 [1, 22]. The α1 subunit of Cav2.1

channel is encoded by the *Cacna1a* gene at the tottering (*tg*) locus of chromosome 8 [5]. Mutations in the *Cacna1a* gene cause several neurologic disorders in humans that have an autosomal-dominant inheritance pattern, including familial hemiplegic migraine, episodic ataxia type 2, and spinocerebellar ataxia type 6 [15].

Cacna1a mutant mice include rocker (*rkr*), tottering (*tg*), rolling Nagoya (*rol*), leaner (*la*), tottering-4j, tottering-5j, wobbly, and pogo mice [3, 9, 11, 16, 23, 24]. These animals display neurologic disorders similar to those observed in humans [22] and are characterized by mild to severe ataxia, movement disorders, and epilepsy [14] and by abnormal expression patterns of calbindin D-28K (Calb1) [9, 18], calretinin (Calb2) [2, 13, 23], tyrosine hydroxylase (TH) [3, 11, 17, 23], zebrin II (Ze-

Table 1. Sequences of primers in this study

Gene	Accession number		Sequences (5'-3')
Calb1	MN_009788.4	Sense	CCTTTGTGGATCAATATGGACAGA
		Antisense	TCAGTTGCTGGCATCGAAAG
Calb2	MN_007586	Sense	ATGGAAGCGGCTATATTGATGAGA
		Antisense	TCGGCCAAGGACATGACAC
Th	MN_009377	Sense	CCGCACATTTGCCCAGTTC
		Antisense	TGCACCGTAAGCCTTCAGCTC
ZebrinII	S72537	Sense	TGCCTGACGGAGACCATGAC
		Antisense	CACCATATTGGGCTTGAGCAGA
Ryr1	X83932.1	Sense	CATCGCCATGGGAGTCAAGA
		Antisense	CAAGTAGACCACTACGGCCAGGA
Ryr2	MN_023868.2	Sense	GCAAGCCAGACTGCATGACC
		Antisense	AAATCGCAATGCCCAGCTTC
Ryr3	MN_177652.2	Sense	ATGACGATGAGCCGGATATGAAG
		Antisense	ACGCCCACGTACATGTGGAA
GAPDH	MN_008084.2	Sense	TGTGTCCGTCGTGGATCTGA
		Antisense	TTGCTGTTGAAGTCGCAGGAG

brinII) [3, 17, 18], ryanodine receptors 1 (Ryr1) [2], ryanodine receptor 2 (Ryr2) [17], and ryanodine receptor 3 (Ryr3) [2] in the cerebellum.

Tottering-6j mice are generated in the Neuroscience Mutagenesis Facility at The Jackson Laboratory (The Jackson Laboratory, Bar Harbor, MA, USA) using ethylnitrosourea administration. In our previous study, we have found that it has a recessive mutation due to a C-to-A base substitution in the *Cacna1a* gene, which leads to exon 5 skipping and consequent direct splicing of exon 4 to exon 6 [10]. Thus, part of the S4-S5 linker, S5, and part of the S5–S6 linker domain are missing in the Cav2.1α1 subunit. We also observed that tottering-6j mice show poor motor coordination [10] and seizure along with its pharmacological profile [7]. However, the protein expression patterns in the cerebellum of tottering-6j mice have not been investigated.

Here we used real-time quantitative reverse transcription polymerase chain reaction (qRT-PCR) and histological methods to determine the expression patterns of proteins in tottering-6j mice, including Calb1, Calb2, TH, ZebrinII, Ryr1, Ryr2, and Ryr3.

Materials and Methods

Ethical declaration

This research was conducted in accordance with the Declaration of Helsinki and was approved by the Animal Experiments Committee of the RIKEN Brain Science Institute (Approved ID: No. H26-2–206). All animals

were cared for and treated humanely in accordance with the Institutional Guidelines for Experiments using Animals.

Animals

The Jackson Laboratory provided the tottering-6j mouse strain, which was generated against a C57BL/6J and BALB/cByJ mixed genetic background [10]. In the present studies, tottering-6j mice were backcrossed with C57BL/6J mice for three generations, producing tottering-6j mice with a C57BL/6J genetic background. The mice were allowed *ad libitum* access to water and food pellets (5058 PicoLab Mouse Diet 20; LabDiet, St. Louis, MO, USA) and housed at room temperature (23 ± 1°C) with 55 ± 5% humidity under a 12:12-h light-dark cycle (lights on from 8:00 am to 8:00 pm). In this study, we used 8-week-old male littermates of tottering-6j mice and wild-type (+/+) mice.

Real-time qRT-PCR

The mice were euthanized with an overdose of pentobarbital sodium. Total RNA was isolated from the cerebellum of 8-week-old mice using TRIzol reagent (Invitrogen, Carlsbad, CA, USA). Five mice were included in each group. To quantify the mRNA levels of the genes of interest, we performed real-time qRT-PCR using an ABI 7700 Sequence Detection System (Applied Biosystems, Waltham, MA, USA), and primers specific to each gene (Table 1). Each PCR mixture contained 8.5 μl sterile water, 12.5 μl SYBR Green (Applied Biosys-

tems), 2 μl cDNA (500 ng/μl), 1 μl forward primer (10 pM/μl), and 1μl reverse primer (10 pM/μl). PCR was performed with an initial denaturation at 95°C for 30 s, followed by 40 cycles, each comprising 95°C for 5 s and 60°C for 30 s. All samples were analyzed in duplicate, and the threshold cycle (Ct) value, which reflects the amount of PCR product, was calculated. The relative levels of mRNA expression were determined based on the Ct values after normalization to glyceraldehyde 3-phosphate dehydrogenase (*GAPDH*), a housekeeping gene. Each mRNA expression level in tottering-6j mice was calculated relative to that of control +/+ mice.

Immunohistochemistry

Mice were anesthetized with an intraperitoneal (i.p.) injection of Nembutal (50 mg/kg). They then were fixed by transcardiac perfusion with 4% paraformaldehyde in phosphate-buffered saline (PBS; pH 7.4). The brains were removed, embedded in paraffin blocks, and sliced into 4-μm-thick mid-horizontal sections. Five mice were included in each group. The sections were deparaffinized with three changes of xylene and two changes of absolute ethanol. Deparaffinized sections were autoclaved for 10 min at 120°C. The sections were rehydrated and incubated for 30 min in 1% H_2O_2 in methanol. The slides were incubated for 1 h in a blocking solution (5% skim milk). The following primary antibodies were used: mouse monoclonal anti-Cab1 (anti-Calbindin-D-28K Clone CB-955; 1:500; Sigma-Aldrich, St. Louis, MO, USA); rabbit monoclonal anti-Calb2 (1:100; Spring Bioscience, Pleasanton, CA, USA); rabbit monoclonal anti-TH (1:100; Sigma-Aldrich); rabbit polyclonal anti-ZebrinII (1:100; Novus Biologicals, Littleton, CO, USA); mouse monoclonal anti-Ryr1 (1:100; Novus Biologicals); rabbit polyclonal anti-Ryr2 (1:100; Novus Biologicals); and rabbit polyclonal anti-Ryr3 (1:100; Merck Millipore, Billerica, MA, USA). The following secondary antibodies were used: biotin-conjugated antibodies for Calb1 and Ryr3 staining; Histofine Simple Stain Mouse MAX PO (Nichirei Biosciences Inc., Tokyo, Japan) for Calb2, TH, ZebrinII, and Ryr2 staining; and polyclonal goat anti-rabbit immunoglobulins/horseradish peroxidase for Ryr1 staining. All slides were subjected to 3,3′-diaminobenzidine histochemistry after secondary antibody incubation.

Cresyl violet and Terminal deoxynucleotidyl transferase-mediated dUTP digoxigenin nick-end-labeling (TUNEL) stainings

Mice were anesthetized with an i.p. injection of Nembutal (50 mg/kg) and then fixed by transcardiac perfusion with 4% paraformaldehyde in PBS (pH 7.4). The brains were removed, embedded in paraffin blocks, and sliced into 4-μm-thick mid-horizontal sections. Five mice were included in each group. The sections were deparaffinized with three changes of xylene and two changes of absolute ethanol. For cresyl violet staining, the slide-mounted brain sections were incubated with cresyl violet (Sigma-Aldrich) for 30 min at 37°C. An ethanol solution was used to differentiate the stain. The sections were then rinsed with distilled water and air-dried fully. TUNEL staining was performed according to the manufacturer's suggested protocol (NeuroTACS[TM]II In Situ Apoptosis Detection Kit; Trevigen, Inc., Gaithersburg, MD, USA).

Quantification of Purkinje cells and granular cells

We counted Purkinje cells in defined areas of cerebellum in a blinded manner. Four square counting frames (1 mm × 1 mm) were placed of the four regularly spaced sections. The number of Purkinje cells and granular cells in each counting frame and the average number was used for statistical analysis in all animals. Five mice were included in each group.

Statistical analysis

The data are presented as the mean ± SEM. Statistical analyses were conducted using Excel Statistics 2006 (SSRI, Tokyo, Japan). The data were analyzed using Dunnett's tests. The results were considered to be statistically significant at a $P<0.05$ or lower probability of error.

Results

mRNA expression patterns in the cerebellum of tottering-6j mice

We assessed the expression patterns of *Calb1*, *Calb2*, *TH*, *ZebrinII*, *Ryr1*, *Ryr2*, and *Ryr3* mRNA in the mouse cerebellum using real-time qRT-PCR analysis (Fig. 1). The expression of *TH*, *ZebrinII*, and *Ryr3* mRNA was significantly increased in tottering-6j mice compared with that of +/+ mice. Conversely, the transcript levels of *Calb2* were significantly decreased in tottering-6j mice in comparison with +/+ mice. No amplification
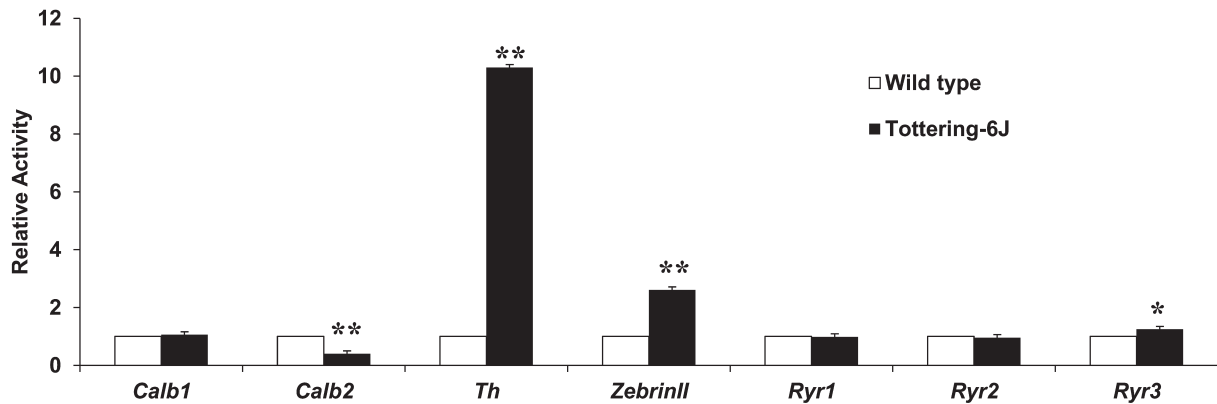
Fig. 1. mRNA expression of calbindin D-28K (*Calb1*), calretinin (*Calb2*), tyrosine hydroxylase (*TH*), Zebrin II (*ZebrinII*), ryanodine receptor 1 (*Ryr1*), ryanodine receptor 2 (*Ryr2*), and ryanodine receptor 3 (*Ryr3*) genes in the cerebellum of wild-type and tottering-6j mice. The data are presented as means ± SEM. * $P<0.05$, ** $P<0.01$, compared with the appropriate control (Dunnett's test).

products were detected in the fractions that did not include cDNA (data not shown).

Histological observation of protein expression patterns in the cerebellum of tottering-6j mice

We have used cresyl violet staining to check the gross morphology and cytoarchitecture. The gross morphology (data not shown) and cytoarchitecture (Fig. 2) of the cerebellum in tottering-6j mice were similar to those of +/+ mice. The numbers of Purkinje cells between +/+ and tottering-6j mice showed no significant difference (+/+; 37 ± 5 cells/mm², *tottering-6*; 41 ± 3 cells/mm², $P>0.05$). The numbers of granule cells between +/+ and tottering-6j mice also showed no significant difference (+/+; 2,965 ± 35 cells/mm², tottering-6; 2,970 ± 120 cells/mm², $P>0.05$).

We determined the expression levels of Calb1, Calb2, TH, ZebrinII, Ryr1, Ryr2, and Ryr3 in the cerebellum of +/+ and tottering-6j mice using immunostaining. The expression levels of Calb1, Ryr1, and Ryr2 were similar between +/+ and tottering-6j mice (data not shown). However, the levels of TH (Fig. 3), ZebrinII (data not shown), and Ryr3 (Fig. 4) were higher than those observed in +/+ mice. Specifically, the expressions of TH and ZebrinII were dramatically increased in the Purkinje cells of tottering-6j mice. The Ryr3 expression was increased in the granular layer of tottering-6j mice. Despite the abovementioned increased protein expression levels in tottering-6j mice, the level of Calb2 was lower than that observed in the granular layer of the cerebellum in +/+ mice (Fig. 5).

Apoptotic cell death in the cerebellum of tottering-6j mice

We examined the amount of apoptosis in the cerebellum of +/+ and tottering-6j mice. Apoptotic cell death was observed in the granular layer of the cerebellum in tottering-6j mice. The number of apoptotic cells was greater in tottering-6j mice than in +/+ mice (Fig. 6).

Discussion

In this study, we examined the gross morphology and cytoarchitecture of the cerebellum in tottering-6j mice. While wobbly mice showed shorter length between the molecular layers in cerebellum than +/+ mice [23], tottering-6j mice had normal gross morphology and cytoarchitecture. This finding corresponds with a previous study [10].

Using real time qRT-PCR and immunohistochemistry, we investigated the mRNA and protein expression patterns of *Calb1*, *Calb2*, *TH*, *ZebrinII*, *Ryr1*, *Ryr2*, and *Ryr3* in the cerebellum of tottering-6j mice. The expression of *TH*, *ZebrinII*, and *Ryr3* was significantly increased in tottering-6j mice compared with that of +/+ mice. The expression of *Calb2* was significantly decreased in tottering-6j mice in comparison with +/+ mice. The expression levels of *Calb1*, *Ryr1*, and *Ryr2* were similar between +/+ and tottering-6j mice. These expression patterns were similar between real time qRT-PCR and immunohistochemistry studies. Our results indicated that the alternated Ca²⁺ signaling through mutated Cav2.1 in tottering-6j strain would affect the transcrip-
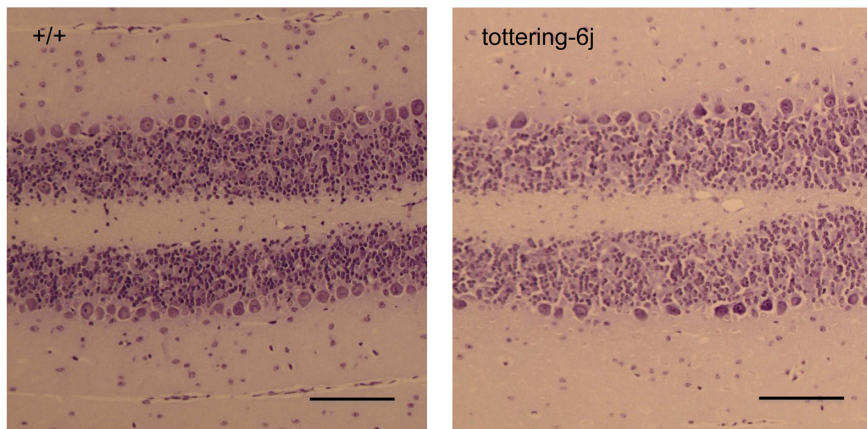
Fig. 2. Cytoarchitecture of the cerebellum. Tottering-6j mice had normal cytoarchitecture compared with +/+ mice. There was no Purkinje cell degeneration, and the length of the molecular layer was normal. The scale bar represents 200 μm.
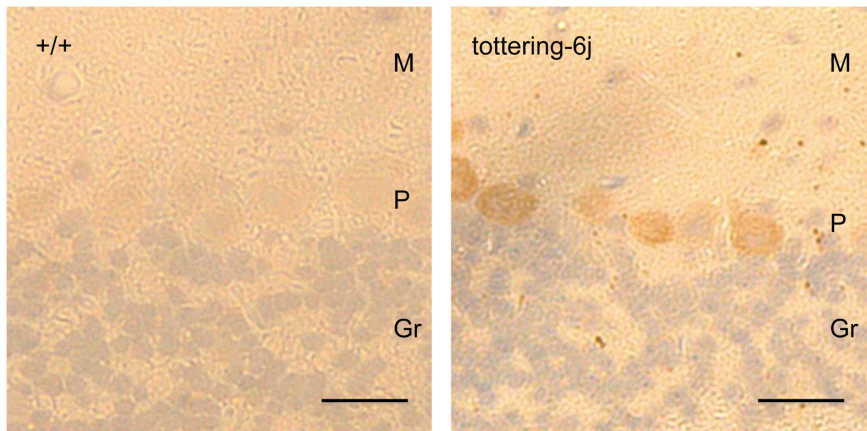

Fig. 3. Expression of TH in the cerebellum. TH expression was increased in the cerebellum of tottering-6j mice compared with +/+ mice. The scale bar represents 50 μm. M: molecular layer, P: Purkinje cell layer, Gr: granular layer.
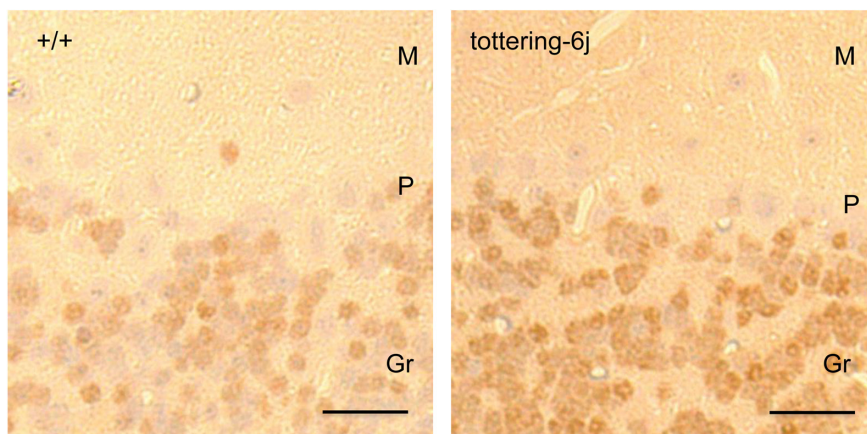

Fig. 4. Expression of Ryr3 in the cerebellum. Ryr3 expression was increased in tottering-6j mice compared with +/+ mice. The scale bar represents 50 μm. M: molecular layer, P: Purkinje cell layer, Gr: granular layer.
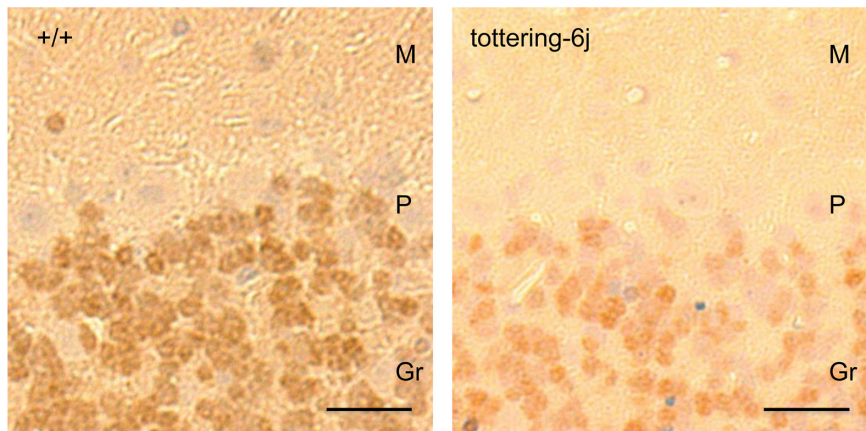
Fig. 5. Expression of Calb2 in the cerebellum. Calb2 expression was decreased in tottering-6j mice compared with +/+ mice. The scale bar represents 50 μm. M: molecular layer, P: Purkinje cell layer, Gr: granular layer.
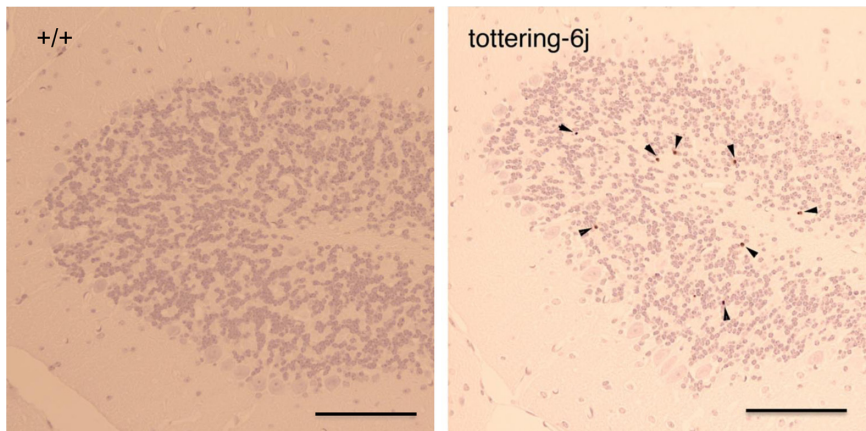

Fig. 6. Apoptotic cell death in the cerebellum. The number of apoptotic cells in tottering-6j mice was greater than that of +/+ mice. Apoptotic cells were found in the granular layer. Apoptotic cells are indicated with arrowheads. The scale bar represents 200 μm.

tional mechanisms for controlling expression of the *Calb2*, *TH*, *ZebrinII*, and *Ryr3* in the cerebellum.

Calb1 and Calb2 are calcium-binding proteins that are enriched in cerebellar cells [19, 20]. Calb1 is predominantly expressed in Purkinje cells. Granule cells are the predominant neuron type that expressed Calb2 [19]. Calb1 expression was found to be decreased in some *Cacna1a* mutant strains, including *tg* [16] and pogo [9] mice, indicating the loss of Purkinje cells. Calb1 expression was normal in tottering-6j mice, which supports the concept that tottering-6j mice do not exhibit Purkinje cell degeneration. *tg*, wobbly, and *la* mice exhibited a significant reduction in the expression of Calb2 in the granular layer [2, 13, 23]. Tottering-6j mice also showed attenuated Calb2 expression in the granular cells. A pre-

vious study reported the absence of Calb2 in the cerebellar granule cells of *Calb2* −/− mice, which displayed altered Purkinje cell firing that resulted in impaired motor coordination [20]. These results indicate that *Cacna1a* mutation would lead to abnormal signal communication between granular and Purkinje cells and result in ataxia.

TH is a key enzyme involved in the Cav2.1 related noradrenergic biosynthesis pathway [3]. In this study, a specific subset of Purkinje cells in 8-week-old tottering-6j mice exhibited persistent TH expression which is not expressed in +/+ mice. This result correlates with our previous study [10]. Abnormal expression of TH was also found in other *Cacna1a* mutant mice, including *la* [3], *tg* [3], *rol* [16], tottering-4j [11], tottering-5j [11],

and wobbly [23]. ZebrinII is predominantly expressed in Purkinje cells, but little is known about its functional significance [3]. The expression pattern of TH resembles that of ZebrinII, a late-onset pattern marker, in *tg*, *la*, and *rol* mice [3, 16, 18]. Its expression pattern consists of an array of parasagittal stripes, each comprising a few hundred to a few thousand Purkinje cells [8]. A similar expression pattern of TH and ZebrinII was found in tottering-6j mice. The level of the ZebrinII signal was also enhanced in tottering-6j mice.

Ryrs are channels involved in intracellular calcium release [17]. Three types of Ryrs have been identified and are widely expressed in mouse tissues [4]. Ryr1 expression was observed in Purkinje cells, whereas Ryr3 expression is found in granule cells [4, 12]. Sawada *et al.* (2008) suggested that Cav2.1 channel dysfunction might affect Ryr1 and Ryr3 expression via altered Ca^{2+} concentration in cerebellar neurons [17]. There are several reports of altered Ryr expression in *Cacna1a* mutant mice. Ryr1 expression was decreased in the cerebellum of *tg* mice [2]. *Rol* mice displayed a reduced Ryr1 expression signal and an enhanced Ryr3 expression signal [17]. In tottering-6j mice, the expression of Ryr1 and Ryr2 was similar to that of +/+ mice. The reason for normal Ryr1 expression is unclear in the present study. We assume that the location of the mutation in the $Cav2.1\alpha_1$ subunit of tottering-6j mice does not affect Ryr1 expression; however, the location of the mutation in *tg* and *rol* mice does.

The cerebellum undergoes apoptosis during normal development. This process ends around postnatal day 17 [6]. TUNEL-positive cells were frequently found in the granule cell layer of tottering-6j mice, similar to *rol* [21] and *la* mice [3]. Similar to other mutant mice, cerebellar maturation would also be delayed in tottering-6j mice.

In summary, the results from this study showed the expression patterns of Calb1, Calb2, TH, ZebrinII, Ryr1, Ryr2, and Ryr3 in the cerebellum of tottering-6j mice in comparison with other *Canca1a* mutant mice. These expression patterns were the result of Ca^{2+} dysregulation due to the mutation in the *Cacna1a* gene. The mutation locations differ in each mutant mouse strain. Therefore, the expression patterns might be different among mutant mice. We showed that differences in the location of the *Cacna1a* mutation play a significant role in mRNA and protein expression patterns and that similar to mutant mouse strains, mutation locations differ in human neurologic disorders, such as familial hemiplegic migraine,

episodic ataxia type 2, and spinocerebellar ataxia type 6. Although seven would be a very small number of proteins to be considered as 'profile' to probe human neurologic disorder, our findings could be useful in studies of mRNA and protein expressions. Thus, the tottering-6j strain is a useful model for cerebellar mRNA and protein expression studies of the Cav2.1 dependent Ca^{2+} signaling.

Acknowledgments

References

1. Catterall, W.A. 1998. Structure and function of neuronal Ca^{2+} channels and their role in neurotransmitter release. *Cell Calcium* 24: 307–323. [Medline] [CrossRef]
2. Cicale, M., Ambesi-Impiombato, A., Cimini, V., Fiore, G., Muscettola, G., Abbott, L.C., and de Bartolomeis, A. 2002. Decreased gene expression of calretinin and ryanodine receptor type 1 in tottering mice. *Brain Res. Bull.* 59: 53–58. [Medline] [CrossRef]
3. Fletcher, C.F., Lutz, C.M., O'Sullivan, T.N., Shaughnessy, J.D. Jr., Hawkes, R., Frankel, W.N., Copeland, N.G., and Jenkins, N.A. 1996. Absence epilepsy in tottering mutant mice is associated with calcium channel defects. *Cell* 87: 607–617. [Medline] [CrossRef]
4. Giannini, G., Conti, A., Mammarella, S., Scrobogna, M., and Sorrentino, V. 1995. The ryanodine receptor/calcium channel genes are widely and differentially expressed in murine brain and peripheral tissues. *J. Cell Biol.* 128: 893–904. [Medline] [CrossRef]
5. Green, M.C.1996. Catalog of mutant genes and polymorphic loci. pp. 12–403. *In*: Genetic variants and Strains of the laboratory mouse. (Lyon, M.F. Searle, A.G. eds.), Oxford University Press, Oxford.
6. Hashimoto, K. and Kano, M. 2013. Synapse elimination in the developing cerebellum. *Cell. Mol. Life Sci.* 70: 4667–4680. [Medline] [CrossRef]
7. Kim, T.Y., Maki, T., Zhou, Y., Sakai, K., Mizuno, Y., Ishikawa, A., Tanaka, R., Niimi, K., Li, W., Nagano, N., and Takahashi, E. 2015. Absence-like seizures and their pharmacological profile in tottering-6j mice. *Biochem. Biophys. Res. Commun.* 463: 148–153. [Medline] [CrossRef]
8. Larouche, M. and Hawkes, R. 2006. From clusters to stripes: the developmental origins of adult cerebellar compartmentation. *Cerebellum* 5: 77–88. [Medline] [CrossRef]
9. Lee, N.S. and Jeong, Y.G. 2009. Pogo: a novel spontaneous ataxic mutant mouse. *Cerebellum* 8: 155–162. [Medline] [CrossRef]

10. Li, W., Zhou, Y., Tian, X., Kim, T.Y., Ito, N., Watanabe, K., Tsuji, A., Niimi, K., Aoyama, Y., Arai, T., and Takahashi, E. 2012. New ataxic tottering-6j mouse allele containing a Cacna1a gene mutation. *PLoS ONE* 7: e44230. [Medline] [CrossRef]

11. Miki, T., Zwingman, T.A., Wakamori, M., Lutz, C.M., Cook, S.A., Hosford, D.A., Herrup, K., Fletcher, C.F., Mori, Y., Frankel, W.N., and Letts, V.A. 2008. Two novel alleles of tottering with distinct Ca(v)2.1 calcium channel neuropathologies. *Neuroscience* 155: 31–44. [Medline] [CrossRef]

12. Mori, F., Fukaya, M., Abe, H., Wakabayashi, K., and Watanabe, M. 2000. Developmental changes in expression of the three ryanodine receptor mRNAs in the mouse brain. *Neurosci. Lett.* 285: 57–60. [Medline] [CrossRef]

13. Nahm, S.S., Tomlinson, D.J., and Abbott, L.C. 2002. Decreased calretinin expression in cerebellar granule cells in the leaner mouse. *J. Neurobiol.* 51: 313–322. [Medline] [CrossRef]

14. Pietrobon, D. 2002. Calcium channels and channelopathies of the central nervous system. *Mol. Neurobiol.* 25: 31–50. [Medline] [CrossRef]

15. Pietrobon, D. 2010. CaV2.1 channelopathies. *Pflugers Arch.* 460: 375–393. [Medline] [CrossRef]

16. Sawada, K., Kalam Azad, A., Sakata-Haga, H., Lee, N.S., Jeong, Y.G., and Fukui, Y. 2009. Striking pattern of Purkinje cell loss in cerebellum of an ataxic mutant mouse, tottering. *Acta Neurobiol. Exp. (Wars.)* 69: 138–145. [Medline]

17. Sawada, K., Hosoi, E., Bando, M., Sakata-Haga, H., Lee, N.S., Jeong, Y.G., and Fukui, Y. 2008. Differential alterations in expressions of ryanodine receptor subtypes in cerebellar cortical neurons of an ataxic mutant, rolling mouse Nagoya. *Neuroscience* 152: 609–617. [Medline] [CrossRef]

18. Sawada, K., Sakata-Haga, H., and Fukui, Y. 2010. Alternating array of tyrosine hydroxylase and heat shock protein 25 immunopositive Purkinje cell stripes in zebrin II-defined transverse zone of the cerebellum of rolling mouse Nagoya. *Brain Res.* 1343: 46–53. [Medline] [CrossRef]

19. Schwaller, B., Meyer, M., and Schiffmann, S. 2002. 'New' functions for 'old' proteins: the role of the calcium-binding proteins calbindin D-28k, calretinin and parvalbumin, in cerebellar physiology. Studies with knockout mice. *Cerebellum* 1: 241–258. [Medline] [CrossRef]

20. Schwaller, B. 2014. Calretinin: from a "simple" Ca(2+) buffer to a multifunctional protein implicated in many biological processes. *Front Neuroanat* 8: 3. [Medline] [CrossRef]

21. Suh, Y.S., Oda, S., Kang, Y.H., Kim, H., and Rhyu, I.J. 2002. Apoptotic cell death of cerebellar granule cells in rolling mouse Nagoya. *Neurosci. Lett.* 325: 1–4. [Medline] [CrossRef]

22. Takahashi, E. 2012. Cav2.1 channelopathy and mouse genetic approaches to investigate function and dysfunction of Cav2.1 channel. pp. 149–158. *In*: Calcium signaling. (Yamahuchi, M. ed.), Nova Science Publishers, Inc., New York.

23. Xie, G., Clapcote, S.J., Nieman, B.J., Tallerico, T., Huang, Y., Vukobradovic, I., Cordes, S.P., Osborne, L.R., Rossant, J., Sled, J.G., Henderson, J.T., and Roder, J.C. 2007. Forward genetic screen of mouse reveals dominant missense mutation in the P/Q-type voltage-dependent calcium channel, CACNA1A. *Genes Brain Behav.* 6: 717–727. [Medline] [CrossRef]

24. Zwingman, T.A., Neumann, P.E., Noebels, J.L., and Herrup, K. 2001. Rocker is a new variant of the voltage-dependent calcium channel gene Cacna1a. *J. Neurosci.* 21: 1169–1178. [Medline]